Theoretical study of the nonpolar surfaces and their oxygen passivation in 4*H*- and 6*H*-SiC

E. Rauls,[1] Z. Hajnal,[1,2] P. Deák,[3] and Th. Frauenheim[1]
[1]*Universität Paderborn, Fachbereich Physik, Theoretische Physik, Warburger Strasse 100, D-33100 Paderborn, Germany*
[2]*MTA Research Institute for Technical Physics and Materials Science, P.O.B. 49, H-1525 Budapest, Hungary*
[3]*Department of Atomic Physics, TU Budapest, Budafoki út 8, H-1111 Budapest, Hungary*
(Received 27 April 2001; revised manuscript received 26 July 2001; published 4 December 2001)

Structure and stability of nonpolar surfaces in 4H- and 6H-SiC have been investigated within the framework of a self-consistent charge density functional based tight binding method. The lowest energy stoichiometric surface is corrugated for $(10\bar{1}0)$ but atomically smooth for $(11\bar{2}0)$. The most stable clean surfaces are Si rich, independent of the growth conditions. Unlike the polar surfaces both nonpolar surfaces can completely be passivated by a single SiO_2 adlayer.

DOI: 10.1103/PhysRevB.64.245323 PACS number(s): 68.35.Md, 81.65.Mq, 68.35.Bs

I. INTRODUCTION

Silicon carbide is emerging as the best candidate for the semiconductor material of low-loss high-power metal-oxide-semiconductor field-effect transistors (MOSFET's). Among the many polytypes of SiC, hexagonal 4H and 6H crystals grown along the [0001] direction are generally used. The (0001) surface is polar: either carbon or silicon terminated. Recently, it was shown that the nonpolar $(11\bar{2}0)$ surface shows a very smooth surface morphology with extremely low defect density,[1] and MOSFET's fabricated on them have much higher channel mobility—due to a lower interface state density—than devices made on the polar surface.[2]

The structure of a surface on the atomic scale is a key factor to the emerging morphology. The polar surfaces of hexagonal SiC have been sudied extensively in this respect—both experimentally and theoretically (for reviews see Ref. 3). Ideal (0001) surfaces show various complicated reconstruction patterns with a high number of dangling bonds, depending on the environmental conditions. This is a cause for morphological defects. The nonpolar surfaces have received much less attention. Sublimation growth along the nonpolar directions has been investigated experimentally in Ref. 4, showing, e.g., the possibility to obtain micropipe-free crystals. To our knowledge no theoretical work has been done on them yet. The first aim of this paper is to find the lowest energy surface structure of the $(10\bar{1}0)$ and $(11\bar{2}0)$ surfaces. Preliminary results of our study have been published in Ref. 5.

The oxide layer in MOSFET's serves also the passivation of surface dangling bonds of the semiconductor. The structure of the interface is of course affected by the formation of the SiO_2 layer but in first approximation the critical question is whether and how the dangling bonds can be saturated by the first oxygen layer. The second aim of this paper is to compare the various surfaces of 4H and 6H SiC in this respect.

II. METHOD

The surfaces were modelled by slabs with periodic boundary conditions, saturated on the bottom side with hydrogen. For the $(10\bar{1}0)$ slabs three and five double layers of (4×1) 2D cells are considered in 4H- and 6H-SiC, respectively. In the $(11\bar{2}0)$ slabs there are six layers of (2×1) 2D cells included for each polytype (one unit cell along the polar axis). The adstructure on the (0001) surface has been built upon a two by two cell of $(\sqrt{3}\times\sqrt{3})R30°$ unit cells with four bilayers of SiC.

To calculate total energies, the self-consistent charge density-functional based tight-binding method (SCC-DFTB) has been used. A detailed description of SCC-DFTB is given in Refs. 6–8 and first successful applications to SiC surfaces are reported in Refs. 9,10. The coordinates of the atoms of all surface structures have been fully relaxed, keeping the H passivated bottom layer fixed to simulated the presence of the bulk.

The formation energies of the surfaces depend on the chemical potentials μ_i of all the species i in the reservoir where the constituents are taken from. For SiC the formation energies are usually plotted against μ_{Si}, while in equilibrium the other variable μ_C can be expressed through the relation between the chemical potential of the SiC crystal μ_{SiC} and the constituents

$$\mu_{SiC}=\mu_{Si}+\mu_C. \tag{1}$$

This formalism can also be extended to surfaces with impurities in a straightforward manner. The formation energy is now given by

$$E_{form}=E_{structure}-\mu_{SiC(bulk)}n_C-\mu_{Si}(n_{Si}-n_C)-\mu_O n_O. \tag{2}$$

In this equation, the n_i denote the numbers of atoms of type i. Since the first term $E_{structure}$ shall only describe the total energy of the H-free surface of the slab, certain boundary planes have to be used to divide the slab. Thereby, two parts are obtained, one bulk like and one surface like, whereof only the latter is of interest. These boundary planes have to be constructed once for every crystal direction, such that they yield unambigious values for $E_{structure}$. The general formalism of constructing such boundaries has been described in Refs. 11,12.

According to this formalism, the first term $E_{structure}$ is calculated within SCC-DFTB for the particular structure. The

chemical potentials $\mu_{\mathrm{Si}}, \mu_{\mathrm{SiC(bulk)}}$, and μ_{O} are known from former calculations or are being varied in a sensible range, respectively.

In studying ''clean'' surfaces (without oxygen) we have considered the full range of μ_{Si}, from the theoretical limit of Si-rich conditions $\mu_{\mathrm{Si}}=\mu_{\mathrm{Si}}^{\mathrm{bulk}}$, to the theoretical limit of C-rich conditions $\mu_{\mathrm{C}}=\mu_{\mathrm{C}}^{\mathrm{bulk}}$. In case of the oxidation process we have assumed ''stoichiometric'' conditions, i.e.,

$$\mu_{\mathrm{Si}}=\mu_{\mathrm{Si}}^{\mathrm{bulk}}-\frac{1}{2}\Delta H_f^{\mathrm{SiC}}, \tag{3}$$

where $\Delta H_f^{\mathrm{SiC}}$ is the heat of formation of silicon carbide. The source of oxygen in the oxidation process was assumed to be O_2 in equilibrium with the SiC crystal. The chemical potential of oxygen in an O_2 gas depends strongly on the temperature and pressure. We have considered two cases: oxidation under ultravacuum conditions (typically used in surface studies) with an oxygen partial pressure of 10^{-5} Torr (1.33×10^{-3} Pa), and normal thermal oxidation under atmospheric conditions, 760 Torr (101325 Pa).

Using the calculated total energy of the oxygen molecule $E(\mathrm{O_2})=-178.14$ eV, the chemical potential of oxygen can be obtained from the formula of Ref. 13 as the function of temperature

For $p=1.33\times10^{-3}$ Pa:

$$\mu_{\mathrm{O}}(T)=-89.07+4.309\times10^{-5}T \times\ln\left(\frac{4.397\times10^{-11}}{T^{(7/2)}}(1-e^{-2260/T})\right)+9.05\times10^{-17}. \tag{4}$$

For $p=101325$ Pa:

$$\mu_{\mathrm{O}}(T)=-89.07+4.309\times10^{-5}T \times\ln\left(\frac{3.341\times10^{-3}}{T^{(7/2)}}(1-e^{-2260/T})\right)+9.05\times10^{-17}, \tag{5}$$

where T is in [K] and μ_{O} is in [eV]. Note that temperature effects are only taken into account in μ_{O} of the gas phase, while entropy effects (in the order of 10^{-4} eV/K per SiO_2 formula unit) are neglected in the solid phase. To account for differently sized surface cells, we plotted in the energy diagrams the formation energy E_{form}, calculated as in Eq. (2), divided by the respective surface area.

III. RESULTS

A. Structure and stability of the clean surfaces

(10$\bar{1}$0) surfaces. For all the hexagonal atoms, structures on the [10$\bar{1}$0] surface may have one (''type I'') or two (''type II'') dangling bonds. In 2H-SiC, surfaces consisting only of type I or type II atoms can be created,[9] see Fig. 1. From simple bond counting arguments one expects surfaces of type II to be less stable than those with type I atoms. This has already been shown quantitatively for the 2H-(10$\bar{1}$0) surface.[9] In 4H- and 6H-SiC all surface structures containing type II elements turned out to be unstable, with respect to the other ones as well.

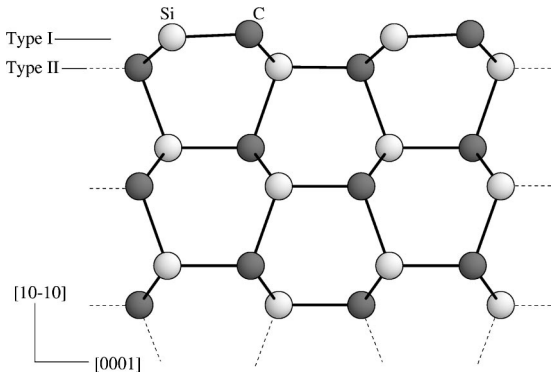

FIG. 1. Schematic side view of a 2H-(10$\bar{1}$0) surface. There are two different types of surfaces in the {10$\bar{1}$0} direction, as indicated in the figure. The same distiction can be made for (10$\bar{1}$0) surfaces in 4H and 6H material.

For the (10$\bar{1}$0)-surface in 4H-SiC there are three inequivalent possibilities to cut the bulk. These three cuts (denoted as *A*,*B*, and *C*) are indicated with horizontal lines in Fig. 2 (left). The surface cuts *B* and *C* consist of two type I and two type II surface atoms per unit cell. In surface *A*, there are only type I atoms, i.e., two dangling bonds less per unit cell compared to *B* and *C*. Accordingly, the energies of *B* and *C* are much higher than that of *A*. Thus, the ideal surface in 4H-SiC is a non planar surface consisting only of threefold coordinated surface atoms. A side view of the relaxed ideal 4H surface as obtained by a cut along *A* is shown in Fig. 2. We determined the absolute energy of the relaxed ideal surface to be 224 meV/Å^2 (3.61 J/m^2).

In the 6H polytype there are four inequivalent possibilities to make a (10$\bar{1}$0) cut, see Fig. 3, but none of them creates a surface with only type I atoms. Nevertheless, such a surface can be obtained by a nonplanar cut along the dashed line shown in Fig. 3. This cut yields a nonplanar surface consisting only of surface atoms with one dangling bond each. Therefore, this is the most stable ideal (10$\bar{1}$0) surface in

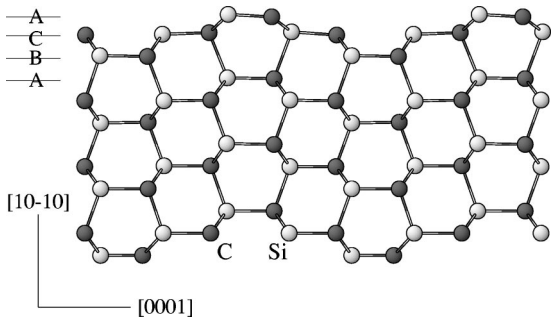

FIG. 2. Schematic side view of the clean 4H-(10$\bar{1}$0) surface. There are three inequivalent possibilities (denoted *A*,*B*,*C*) to create a (10$\bar{1}$0) surface. On the top side the relaxed ideal surface created by cut *A* is shown.

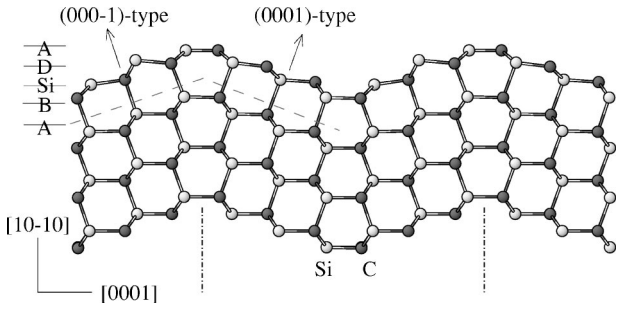

FIG. 3. Schematic side view of the clean 6H-$(10\bar{1}0)$ surface. There are four inequivalent surface cuts (denoted A,B,C,D) to create a $(10\bar{1}0)$ surface. The ideal surface, obtained by the nonplanar cut A, can also be seen as a facetted surface. The facets are alternately (0001)- and $(000\bar{1})$-surface segments. The dashed lines mark the segment shown for the adstructures in Fig. 5.

6H-SiC. As its construction suggests, it can also be regarded as a facetted surface consisting alternately of (0001)- and $(000\bar{1})$-surface segments. Reflecting on the most stable reconstructions of these polar surfaces[14,15] it can be seen, that they cannot be formed in this case to stabilize the facetted planes, for their periodicity is too large and a rotation of the unit cell [e.g., as in the $(\sqrt{3}\times\sqrt{3})R30°$-reconstruction] is prohibited by the given direction of the neighbored facettes. The energy of the relaxed ideal surface was found to be 232 meV/Å^2 (3.74 J/m^2).

The clean $(10\bar{1}0)$ surface is metallic both in 4H- and 6H-SiC, explaining the higher energies compared to the $(10\bar{1}0)$ surface in 2H-SiC ($\approx$188 meV/Å^2).[9] As outlined below, this is a consequence of the geometrical structure. Usually, on nonpolar SiC surfaces, the Si atoms move inward and the C atoms move outward from the surface. The reason is a charge transfer: the Si dangling bond, which has a high energy, emits charge to the lower lying C dangling bond. The surface cation which has lost an electron favours a more planar sp^2-like hybridization, while the surface anion moves outward in a p^3 configuration. The resulting configuration can thus lower its energy. For the $(10\bar{1}0)$ surface in 2H-SiC, this mechanism works fine, but it cannot be simply transferred to 4H- and 6H-SiC, becuse of the constraints posed by the ideal $(10\bar{1}0)$ surfaces there. For the topmost two surface atoms, the situation is the same as for the surface atoms in the corresponding 2H surface. They are both neighbor to two bulk atoms and one surface atom. However, the other two surface atoms have only fourfold coordinated neighbors that cannot relax so easily. For the 6H surface, the situation is even worse, since there are two more atoms per unit cell, which cannot follow the easy relaxation mechanism because of having fourfold coordinated neighbors only. Therefore, a buckling reconstruction of the ideal $(10\bar{1}0)$ surface in 4H- and 6H-SiC is not possible.

It should be noted that the ideal relaxed $(10\bar{1}0)$ surfaces are corrugated on an atomic scale. Defining a surfaces roughness r as

$$\Delta r = z_{\max} - z_{\min}, \tag{6}$$

where z means the position of the surfaces atoms along the surface normal, gives a value of 1.67 Å for the 4H polytype and 2.57 Å for 6H.

The ideal $(10\bar{1}0)$ surfaces still contain one dangling bond per surface atom. Some of them can be saturated assuming a silicon excess on the surface. (Due to its shorter bonds, carbon cannot play this role.) Figures 4(a) and 5(a) show structures where three fourth of the dangling bonds in 4H- and two third in 6H-SiC are saturated. The surface with the Si adstructure is nonmetallic. In 4H-SiC, it consists of buckled dimers of Si adatoms where one atom of the pair has esentially a lone pair and the other an empty dangling bond [left-hand side of Fig. 4(a)]. Similarly the carbon atom in the remaining Si C surface dimers [on the right of Fig. 4(a)] attracts most of the electron from the dangling bond of the Si atom. The Si adstructure lowers the energy over the whole range of the chemical potential of silicon, i.e., even in an extremely carbon rich environment. An energy diagram is given for 4H-SiC in Fig. 6.

$(11\bar{2}0)$ surfaces. The other low-index nonpolar surface in 4H- and 6H-SiC is the $(11\bar{2}0)$ surface, also parallel to the c axis. In contrast to the $(10\bar{1}0)$ surface, there is just one

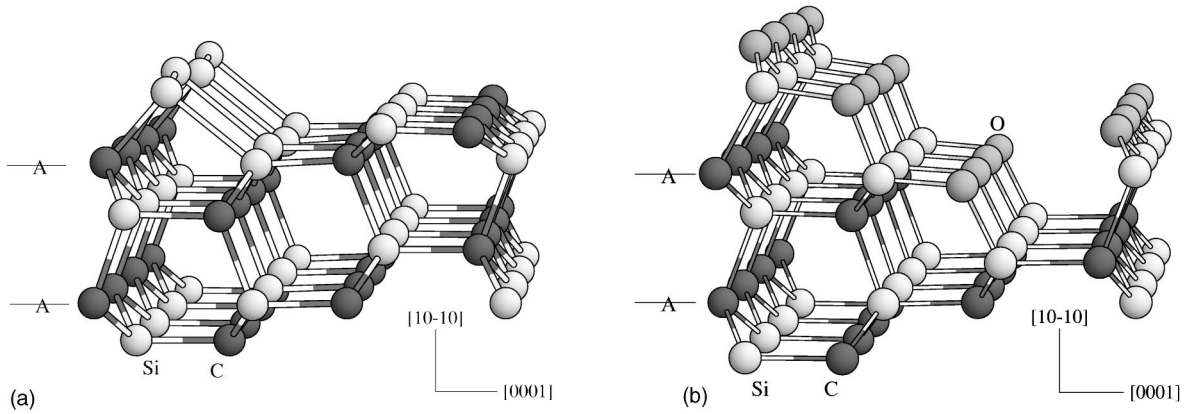

FIG. 4. (a) 4H-$(10\bar{1}0)$ surface with a Si adstructure resulting in a (2×1) reconstruction. (b) This (1×1) SiO adstructure fully passivates the 4H-$(10\bar{1}0)$ surface.

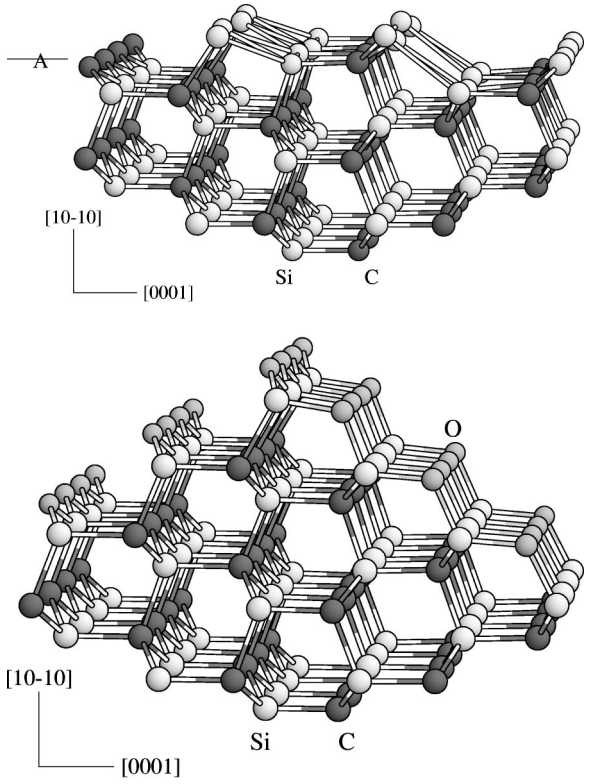

FIG. 5. (a) Si adstructure on the 6H-$(10\bar{1}0)$ surface leading to a (2×1) reconstruction. (b)Fully passivating (1×1) SiO adstructure on the 6H-$(10\bar{1}0)$ surface.

type of $(11\bar{2}0)$ surface in both hexagonal polytypes. The clean $(11\bar{2}0)$ surface in 4H- and 6H-SiC consists of parallel chains of Si and C atoms with one dangling bond each. The geometry of the 4H surface is shown in Fig. 7. The 6H surface is similar except for the shape of the chains and the cell size.

Due to relaxation the surface becomes buckled with the carbon atoms moving upwards and the Si atoms moving towards the bulk. The absolute energy of the relaxed ideal $(11\bar{2}0)$ surface was found to be 208 meV/Å^2 (3.36 J/m^2) and 213 meV/Å^2 (3.43 J/m^2) for the 4H- and the 6H-polytype, respectively.

The relaxed ideal $(11\bar{2}0)$ surfaces are significantly smoother than the $(10\bar{1}0)$ surfaces. With the definition above we find a roughness of only 0.36 Å for 4H- and 0.35 Å for 6H-SiC.

The dangling bonds of the surface atoms on the $(11\bar{2}0)$ surface point 60° out of the surface plane. Since the dangling bonds of neighbored chains point towards each other, they can easily be saturated by putting a chain of adstructure atoms upon this clean surface. We find that a chain of silicon atoms lowers the energy not only under silicon rich but even under extremely carbon rich conditions, see the energy diagram for 4H in Fig. 6. The same structure is obtained by removing the first layer carbon atoms from the ideal surface.

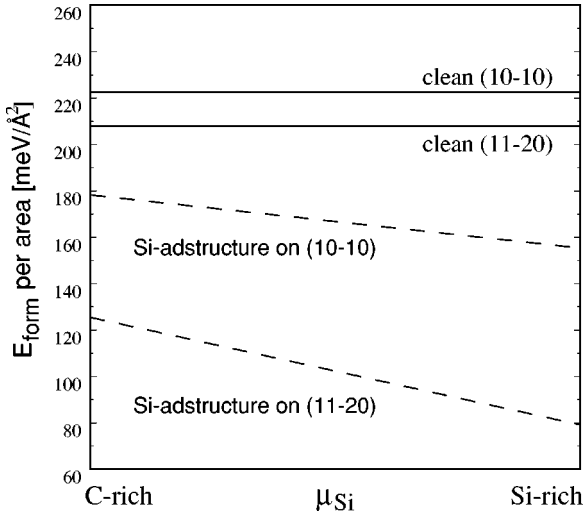

FIG. 6. Comparison of the formation energy E_{form} per area of the 4H$(10\bar{1}0)$ and the 4H$(11\bar{2}0)$ surface with a Si adstructure [see Fig. 4(a)] compared to the clean surfaces in both directions. The construction of the Si adstructure on the $(11\bar{2}0)$ surface is described in the caption of Fig. 7. Over the whole range of the chemical potential of Si the adstructures stabilize both nonpolar surfaces, even under extremely C-rich conditions.

B. Oxidized surfaces

$(10\bar{1}0)$ surfaces. The primary effect of oxidation is passivation of the dangling bonds but obviously an oxygen adlayer may diminish the energy as well. We, therefore, have constructed oxygen adstructures to diminish the number of dangling bonds. In case of the ideal $(10\bar{1}0)$ surfaces complete dangling bond passivation can be achieved. Starting from the ideal surface, and assuming the removal of two rows of carbon atoms (the removal of carbon is expected during oxidizing SiC into SiO_2), one may obtain the structure shown in Fig. 4(b). Here the row of silicon atoms, originally next to the removed carbon rows, is ''relocated'' in a position similar to the Si adstructure and oxygen is inserted into all Si-Si bonds on the surface. An analogous mechanism leads to the oxidized $(10\bar{1}0)$ surface in 6H-SiC as shown in Fig. 5(b).

Although the kinetics of forming such a surface is not considered here, the thermodynamic stability can be estimated by drawing the balance of broken and newly created bonds. Per unit cell of the clean 4H surface, e.g., seven C-Si bonds have to be broken while one new C-Si and eight Si-O bonds are being created. Starting at the top mark ''A'' on the left-hand side of the picture, the structure of the ideal surface can be recognized. In the middle, one row of carbon atoms has been substituted by oxygen atoms, which makes two Si-O bonds per unit cell, but at the same time four C-Si bonds have been removed, since the row of silicon atoms in between has been relocated. On the right a row of threefold coordinated carbon atoms has been replaced by oxygen atoms. This renders two more Si-O bonds per unit cell at the cost of three C-Si bonds. The relocated row of Si atoms on top of the left side of the structure is bridged by further

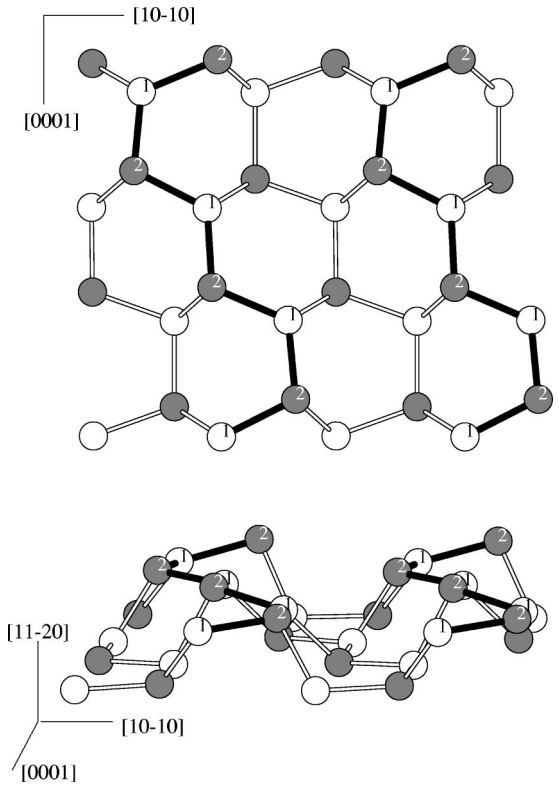

FIG. 7. Top and side view of the ideal $(11\bar{2}0)$ surface in 4H $-SiC$: The surface atoms form parallel chains along the [0001] direction, see black lines. In the relaxed structures these chains become slightly buckled. If the carbon atoms "2"are removed, the Si atoms "1" can form new bonds to the bulk Si atoms. Additionally, weak bonds are created between them as well. The resulting structure is the Si adstructure discussed in the text.

oxygen atoms. Here, one C-Si bond and four Si-O bonds evolve per unit cell. In Fig. 4(b) four unit cells of the adstructure are shown, for better clearness. At the bottom, the structure of the ideal surface can be seen (starting at the bottom mark "A") for comparison. Since the binding energy of Si-O bonds is about 25% higher than that of C-Si bonds, the balance is clearly in favor of this oxidized surface.

The stability of the oxygen passivated $(10\bar{1}0)$ surface of 4H-SiC is compared to the clean ones under UHV oxidation conditions ($p_{O_2}=1.33\times10^{-3}$ Pa) in Fig. 9(a). As can be seen, even at such a low oxygen partial pressure, the surface structure with oxygens is stable up to high temperatures. Obviously this is even more the case in atmospheric oxidation. (Note that the temperature scale should be regarded with some caution, since no temperature effects have been considered on the surface.) The oxygen passivated $(10\bar{1}0)$ surface of 6H-SiC is similarly stable.

The completely passivated $(10\bar{1}0)$ surfaces of 4H- and 6H-Si are even more corrugated than the ideal ones. The roughness Δr is 4.14 Å for the 4H- and 5.88 Å for the 6H-$(10\bar{1}0)$ surface.

$(11\bar{2}0)$ surfaces. The $(11\bar{2}0)$ surfaces of 4H- and 6H-SiC can also be fully passivated by an oxide monolayer. Starting again with the clean surface and removing the carbon atoms from the topmost chain, one ends up with the Si-chain structure described in the preceeding subsection. Inserting oxygen atoms between the Si-atoms in the chain results in the structure shown in Fig. 8(a) for 4H-SiC (and similarly for 6H-SiC). In this structure all the dangling bonds are saturated, but there are still Si-Si bonds left which connect Si atoms of the chain to Si atoms of the second layer. A complete monolayer of SiO_2 adstructure can be obtained, if further O atoms are inserted into all these Si-Si bonds, see Fig. 8(b).

The thermodynamic stability of the oxidized $(11\bar{2}0)$ surfaces are compared with the clean ones in Fig. 9(b) for 4H-SiC in the case of UHV oxidation ($p_{O_2}=1.33\times10^{-3}$ Pa). Although less so than in the case of the $(10\bar{1}0)$ surface, the oxygen adstructures are also stable on the $(11\bar{2}0)$ surface up to sufficiently high temperatures for observation.

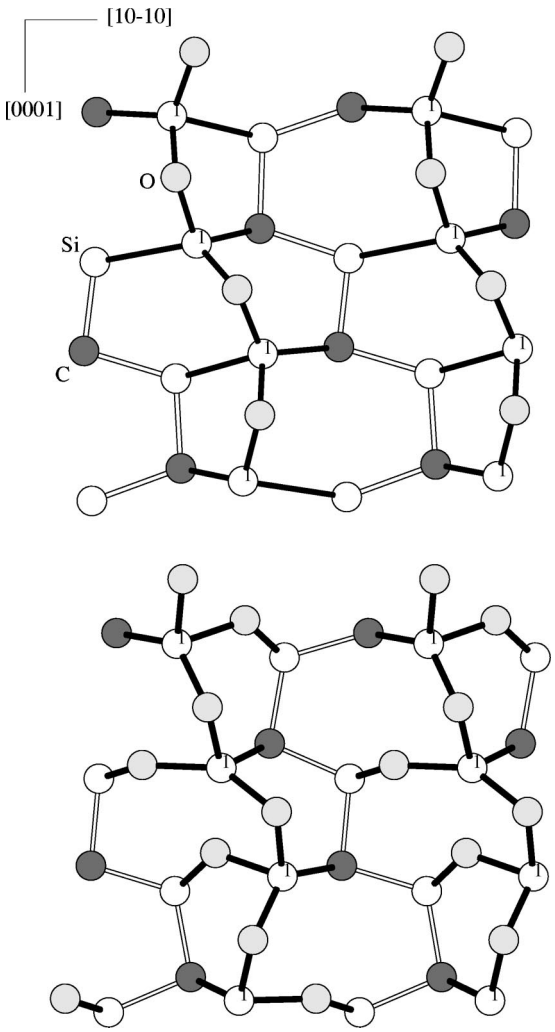

FIG. 8. Two SiO adstructures on top of the $(11\bar{2}0)$ surface in 4H.(a) Starting from the Si adstructure, the construction of which is described in the caption of Fig. 7, oxygen atoms are placed between all the Si atoms "1." In this surface, there are still some Si-Si bonds left. (b) Adding more oxygen to the remaining Si-Si bonds the passivating SiO_2 adstructure is obtained. As a guide to the eye the adstructure chains are emphasized by black lines.

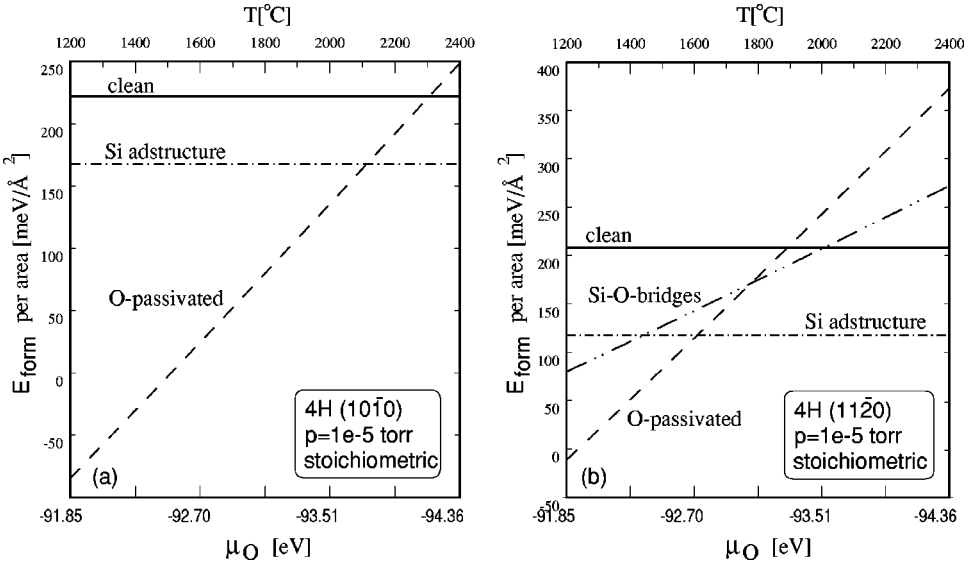

FIG. 9. Stability of the discussed reconstructions of (a) the 4H-$(10\bar{1}0)$ surface and (b) the 4H-$(11\bar{2}0)$ surface depending on the chemical potential μ_O of oxygen and thus, following Eq. (4), on the temperature, see text for details.

IV. DISCUSSION AND COMPARISON WITH THE POLAR SURFACES

Comparing the results for the clean 4H- and 6H-surfaces, we find that they behave similarly but, especially the $(10\bar{1}0)$ surfaces are much more complicated in these two polytypes than in 2H-SiC. The ideal surfaces have a high density of dangling bonds resulting in high formation energies. Adstructures consisting of silicon atoms can lower the energy, so under growth conditions the surface is silicon rich, no matter what the C/Si ratio is. Comparing the $(10\bar{1}0)$ and $(11\bar{2}0)$ surfaces in one polytype, the main difference is in the ''roughness'' on an atomic scale: while the $(10\bar{1}0)$ surface shows a fluctuation in the z coordinate of the topmost atoms within one cell comparable to 100–150% of the Si-C bond length, the $(11\bar{2}0)$ surface is smooth within 15% of the bond length.

Oxygen can completely passivate both surfaces in both polytypes, forming a SiO_2 monolayer stable up to high temperatures even for low oxygen partial pressures. This situation is in contrast to that of the polar (0001) surfaces. There, the surface consists only of Si atoms which form a trigonal lattice. All Si atoms are equivalent and are bonded to three C atoms in the second layer, thus having one dangling bond each pointing perpendicular out of the surface plane. This makes a simple saturation via bridges of Si and O atoms impossible. We find that the best possibility to saturate the surface dangling bonds is the ordered SiO_2 adstructure as proposed in Refs. 16,17. The suggested structure is shown in Fig. 10. On top of two thirds of the surface Si atoms there is a linear Si-O-Si bond, and the topmost Si atoms are connected via O atoms to hexagons. We find that after relaxation the O atoms in the Si-O-Si bonds of the adstructure alternately move to the inside and the outside of the hexagons by 0.27 Å. In this structure there is still one Si dangling bond in each surface unit cell (down the middle of the Si-O rings). Therefore, unlike the nonpolar surfaces, the (0001) surface cannot be fully passivated by a monolayer of SiO_2.

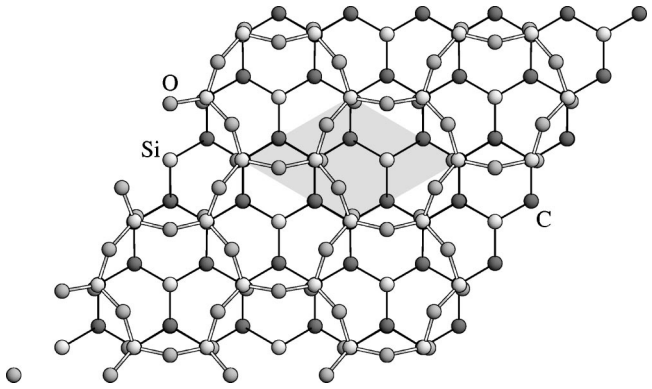

FIG. 10. SiO_2 monolayer on top of the Si-terminated (0001) surface. The structure is a $(\sqrt{3}\times\sqrt{3})R30°$ reconstruction consisting of rings of Si and O atoms that saturate two third of the dangling bonds of the clean surface. Thus one dangling bond per $(\sqrt{3}\times\sqrt{3})R30°$ unit cell remains unsaturated. The shaded region denotes the unit cell.

V. CONCLUSION

We have shown that the ideal $(10\bar{1}0)$ surface of lowest energy is very rough in 4H- and 6H-SiC, while the $(11\bar{2}0)$ surface is exceptionally smooth on an atomic scale. The latter fact may explain the experimentally observed very smooth surface morphology of the nonpolar $(11\bar{2}0)$ surface.[1] We have also shown that, unlike the polar (0001) surface, the nonpolar ones can completely be passivated by oxidation. This may be seen as the reason of the lower interface state density in MOSFETs fabricated on the $(11\bar{2}0)$ surface.[2]

ACKNOWLEDGMENTS

This work was done in the framework of the DFG Project No. FR889/12-1 and the bilateral DFG (Grant No. 436 UNG113/137/0) - MTA (No. 118) project. P.D. also thanks the support of the Hungarian OTKA Grant No. T 032174.

[1] Zhi Ying Chen, T. Kimoto, and H. Matsunami, Jpn. J. Appl. Phys. **38**, L1375 (1999).
[2] H. Yano, T. Hirao, T. Kimoto, and H. Matsunami, Jpn. J. Appl. Phys. **39**, 2008 (2000).
[3] J. Pollmann, P. Krüger, and M. Sabisch, Phys. Status Solidi B **202**, 421 (1997); V. Bermudez, *ibid.*, 447 (1997); U. Starke, *ibid.*, 475 (1997); P.M. Mårtensson, F. Owman, and L.I. Johansson, *ibid.*, 501 (1997).
[4] J. Takahashi and N. Ohtani, Phys. Status Solidi B **202**, 163 (1997).
[5] E. Rauls, Z. Hajnal, P. Deák, and Th. Frauenheim, Mater. Sci. Forum **338-342**, 365 (2000).
[6] J. Elsner, R. Jones, M.I. Heggie, M. Haugk, R. Gutierrez, Th. Frauenheim, S. Öberg and P.R. Briddon, Appl. Phys. Lett. **73**, 3530 (1998).
[7] M. Elstner, D. Porezag, G. Jungnickel, J. Elsner, M. Haugk, Th. Frauenheim, S. Suhai, G. Seifert, Phys. Rev. B **58**, 7260 (1998).
[8] J. Elsner, R. Jones, P.K. Sitch, V.D. Porezag, M. Elstner, Th. Frauenheim, M.I. Heggie, S. Öberg, and P.R. Briddon, Phys. Rev. Lett. **79**, 3672 (1997).
[9] E. Rauls, J. Elsner, R. Gutierrez, and Th. Frauenheim, Solid State Commun. **111**, 459 (1999).
[10] R. Gutierrez, M. Haugk, J. Elsner, G. Jungnickel, M. Elstner, A. Sieck, T. Frauenheim, and D. Porezag, Phys. Rev. B **60**, 1771 (1999).
[11] N. Chetty and R.M. Martin, Phys. Rev. B **45**, 6074 (1992).
[12] K. Rapcewicz, B. Chen, B. Yakobson, and J. Bernholc, Phys. Rev. B **57**, 7281 (1998).
[13] J.E. Northrup, R. Di Felice, and J. Neugebauer, Phys. Rev. B **56**, R4325 (1997).
[14] J.E. Northrup and J. Neugebauer, Phys. Rev. B **52**, R17 001 (1995).
[15] P. Mårtensson, F. Owman, and L.I. Johansson, Phys. Status Solidi B **202**, 501 (1997).
[16] U. Starke, J. Schardt, J. Bernhardt, and K. Heinz, J. Vac. Sci. Technol. A **17**, 1688 (1999).
[17] J. Bernhardt, J. Schardt, U. Starke, and K. Heinz, Appl. Phys. Lett. **74**, 1084 (1999).